JACS
JOURNAL OF THE AMERICAN CHEMICAL SOCIETY

Article

pubs.acs.org/JACS

Rational Synthesis of Low-Polydispersity Block Copolymer Vesicles in Concentrated Solution via Polymerization-Induced Self-Assembly

Carlo Gonzato,[†] Mona Semsarilar,[†] Elizabeth R. Jones,[†] Feng Li,[‡] Gerard J. P. Krooshof,[‡] Paul Wyman,[§] Oleksandr O. Mykhaylyk,*[,†] Remco Tuinier,[‡,∥] and Steven P. Armes*[,†]

[†]Department of Chemistry, The University of Sheffield, Brook Hill, Sheffield, S3 7HF, United Kingdom

[‡]DSM ChemTech Center, Advanced Chemical Engineering Solutions (ACES), P.O. Box 18, 6160 MD Geleen, The Netherlands

[§]DSM Ahead, P.O. Box 18, 6160 MD Geleen, The Netherlands

[∥]Van 't Hoff Laboratory for Physical and Colloid Chemistry, Department of Chemistry, Utrecht University, Padualaan 8, 3584 CH Utrecht, The Netherlands

Supporting Information

ABSTRACT: Block copolymer self-assembly is normally conducted via post-polymerization processing at high dilution. In the case of block copolymer vesicles (or "polymersomes"), this approach normally leads to relatively broad size distributions, which is problematic for many potential applications. Herein we report the rational synthesis of low-polydispersity diblock copolymer vesicles in concentrated solution via polymerization-induced self-assembly using reversible addition−fragmentation chain transfer (RAFT) polymerization of benzyl methacrylate. Our strategy utilizes a binary mixture of a relatively long and a relatively short poly(methacrylic acid) stabilizer block, which become preferentially expressed at the outer and inner poly(benzyl methacrylate) membrane surface, respectively. Dynamic light scattering was utilized to construct phase diagrams to identify suitable conditions for the synthesis of relatively small, low-polydispersity vesicles. Small-angle X-ray scattering (SAXS) was used to verify that this binary mixture approach produced vesicles with significantly narrower size distributions compared to conventional vesicles prepared using a single (short) stabilizer block. Calculations performed using self-consistent mean field theory (SCMFT) account for the preferred self-assembled structures of the block copolymer binary mixtures and are in reasonable agreement with experiment. Finally, both SAXS and SCMFT indicate a significant degree of solvent plasticization for the membrane-forming poly(benzyl methacrylate) chains.

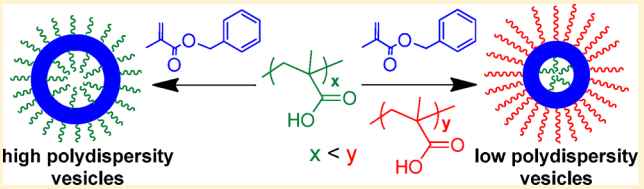

INTRODUCTION

The self-assembly of AB diblock copolymers in selective solvents is a well-known approach for generating a wide range of copolymer morphologies, including spherical micelles, worm-like micelles, or vesicles.[1,2] The latter morphology is of particular interest, since it can be exploited for drug delivery, encapsulation, cosmetics, biomimetic applications, and as nanoreactors.[3−7] Compared with liposomes,[8] block copolymer vesicles exhibit greater toughness, reduced permeability, and less fluid-like membranes.[3,7,9]

Amphiphilic diblock copolymer nano-objects are usually generated via postpolymerization processing using either a solvent switch, pH switch, dialysis, or thin film rehydration; such processing is typically conducted in (mixed) aqueous solution at low copolymer concentrations (typically <1%).[10] The resulting copolymers are often in their frozen, non-ergodic state,[10] in which case the morphologies that are observed are path-dependent. This can be an advantage, because kinetically controlled self-assembly can allow access to various nano-objects from relatively few copolymer compositions. However, this approach can become problematic when a high degree of control over the particle size distribution is desired. This is a particular problem for vesicles, which form via "wrap-up" of planar membranes in solution.[11] Sonication,[12] membrane extrusion,[13] high-pressure homogenization,[14] self-assembly onto a patterned template,[15] or thermal cycling[13] have been used to gain control over vesicle size distributions. In addition, inkjet printing has also been demonstrated to be effective in controlling vesicle size.[16] In the above examples, narrower size distributions are typically achieved, with a concomitant reduction in vesicle dimensions. This is because the interfacial area (and hence interfacial energy) for smaller vesicles is much more size-dependent than for larger vesicles.[17] In addition to such physical processing routes, chemical strategies have also been explored for producing low-polydispersity vesicles. For example, Eisenberg and co-workers reported that, for poly(acrylic acid)-polystyrene (PAA-PS) diblocks, utilizing an artificially broad distribution of PAA block lengths in combination with a fixed degree of polymerization (DP) of the membrane-forming PS block aided the formation of relatively small, low-polydispersity vesicles.[18,19] This was attributed to self-segregation of the PAA chains: longer

Received: May 29, 2014
Published: July 15, 2014

   dx.doi.org/10.1021/ja505406s | J. Am. Chem. Soc. 2014, 136, 11100−11106

Scheme 1. PISA Synthesis of Diblock Copolymer Vesicles via RAFT Dispersion Polymerization of BzMA in Ethanol at 70°C[a]

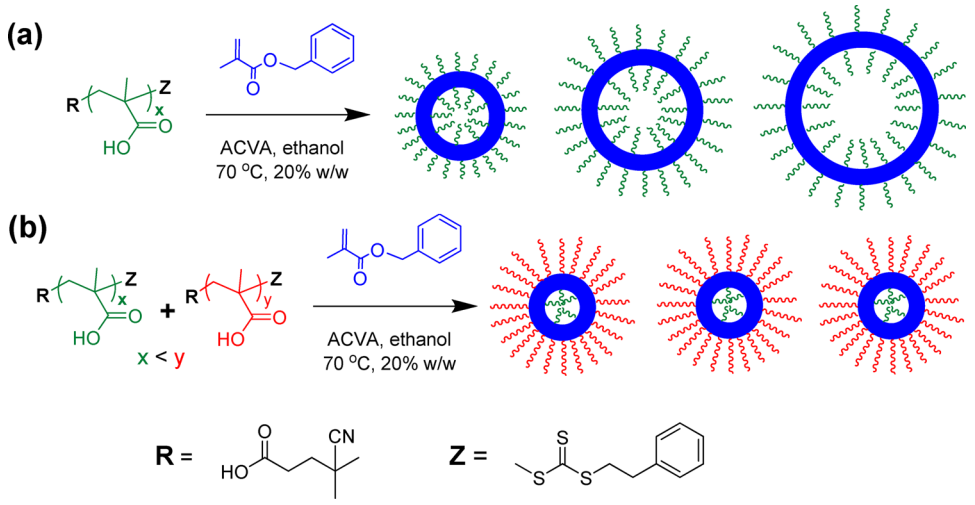

[a](a) chain extension of a single PMAA macro-CTA to give high-polydispersity vesicles; (b) chain extension of two PMAA macro-CTAs having a low (green) and a high (red) mean degree of polymerization, respectively, to produce relatively low-polydispersity vesicles.

chains were preferentially located at the external membrane surface, whereas shorter chains were expressed at the inner membrane surface. This hypothesis was supported by an elegant fluorescence labeling experiment.[19] The feasibility of exerting local thermodynamic control over systems that are globally non-ergodic has been extensively studied both theoretically and experimentally for blends of diblock copolymer amphiphiles[20−26] as well as for asymmetric triblock or tetrablock copolymers.[4,27] Although enhanced control over the vesicular morphology can be achieved using this approach, its multistep nature and the relatively low copolymer concentrations utilized to date constitute major drawbacks with regard to a cost-effective scalable route. However, the recent development of robust polymerization-induced self-assembly (PISA) formulations based on living radical polymerization offers an opportunity to overcome such limitations: vesicles can now be prepared directly in solution at up to 25% solids using either aqueous emulsion[28,29] or alcoholic[30,31] dispersion polymerization. In the present work, we report the *rational* synthesis of low-polydispersity diblock copolymer vesicles via PISA using reversible addition−fragmentation chain transfer (RAFT) dispersion polymerization in concentrated ethanolic solution. In particular, binary mixtures of two poly(methacrylic acid) (PMAA) macromolecular chain transfer agents (macro-CTAs) are chain-extended with benzyl methacrylate (BzMA), see Scheme 1. The resulting diblock copolymer vesicles are characterized using transmission electron microscopy (TEM), dynamic light scattering (DLS), and small-angle X-ray scattering (SAXS). For comparison, PISA syntheses using the individual PMAA macro-CTAs were also performed as control experiments. Finally, we analyzed the thermodynamically preferred self-assembled copolymer vesicle morphologies using self-consistent mean-field theory (SCMFT).

MATERIALS AND METHODS

All reagents were purchased from Sigma-Aldrich (U.K.) and used as received unless otherwise stated. 4,4′-Azobis-4-cyanopentanoic acid (ACVA, >98%) was used as an initiator. Benzyl methacrylate (BzMA, 96%) was passed through a column (supplied by the manufacturer) in order to remove inhibitor prior to use. 4-Cyano-4-(2-phenylethanesulfanylthiocarbonyl)sulfanylpentanoic acid (PETTC) was synthesized as previously reported.[30]

Synthesis of PMAA macro-CTAs. For the typical synthesis of a $PMAA_{62}$ macro-CTA, a round-bottomed flask was charged with MAA (10.0 g; 116 mmol), PETTC (0.607 g; 1.79 mmol), ACVA (0.100 g; 0.36 mmol; PETTC/ACVA molar ratio = 5.0), and ethanol (10.0 g). The sealed flask was cooled using an ice bath and purged with nitrogen gas, then placed in a preheated oil bath at 70 °C for 3 h. The resulting PMAA macro-CTA (MAA conversion =99%; after exhaustive methylation using trimethylsilyl diazomethane, M_n = 6800 g mol^{-1}, M_w = 8800 g mol^{-1}, M_w/M_n = 1.29), was purified by dialysis, first against 9:1 water/methanol and then against deionized water. The polymer was isolated via lyophilization. A mean DP of 62 was calculated for this macro-CTA using ^{1}H NMR spectroscopy by comparing the integrated signal intensity assigned to the aromatic protons at 7.2−7.4 ppm with that due to the methacrylic polymer backbone at 0.4−2.5 ppm. Using this same general protocol, $PMAA_{44}$, $PMAA_{102}$, and $PMAA_{171}$ were synthesized by adjusting the amounts of PETTC and ACVA utilized to achieve the desired target DP (see Table S1 for further details).

Synthesis of poly(methacrylic acid)-poly(benzyl methacrylate) (PMAA-PBzMA) diblock copolymer vesicles by dispersion polymerization in ethanol. In a typical dispersion polymerization targeting $PMAA_{44}$-$PBzMA_{140}$ at 20% w/w solids, BzMA (0.40 g; 2.27 mmol), ACVA (0.90 mg; 0.003 mmol), and $PMAA_{44}$ (0.067 g; 0.016 mmol) were dissolved in ethanol (1.871 g). This reaction mixture was ice-cooled, nitrogen-purged, and placed in a preheated oil bath at 70 °C for 24 h. The monomer conversion was determined by ^{1}H NMR spectroscopy, by comparing the integrated benzyl signal assigned to PBzMA at 4.9 ppm to that of the BzMA vinyl proton signal (CH_2) at 5.2 ppm.

Synthesis of low-polydispersity diblock copolymer vesicles via dispersion polymerization of BzMA in ethanol using a binary mixture of two PMAA macro-CTAs. In a typical dispersion polymerization targeting ($PMAA_{44}$ + $PMAA_{102}$)-$PBzMA_{140}$ at 20% w/w solids, BzMA (0.40 g; 2.27 mmol), ACVA (0.90 mg; 0.003 mmol), $PMAA_{44}$ (0.033 g; 0.008 mmol), and $PMAA_{102}$ (0.074 g; 0.008 mmol) were dissolved in ethanol (2.033 g). The reaction mixture was ice-cooled, purged using nitrogen gas, and placed in a preheated oil bath at 70 °C for 24 h. The polymerization yield was determined by ^{1}H NMR spectroscopy, by comparing the integrated benzyl proton signal assigned to PBzMA at 4.9 ppm to that of the BzMA vinyl signal (CH_2) at 5.2 ppm.

^{1}H NMR Spectroscopy. ^{1}H NMR spectra were acquired in CD_3OD, CD_2Cl_2, $CDCl_3$ or d_6-DMSO using a Bruker 400 MHz spectrometer, with chemical shifts reported in ppm.

Transmission Electron Microscopy (TEM). TEM studies were conducted using a Philips CM 100 instrument operating at 100 kV. TEM samples were prepared as follow: copper-palladium TEM grids (Agar Scientific, U.K.) were surface-coated in-house to yield a thin film

dx.doi.org/10.1021/ja505406s | J. Am. Chem. Soc. 2014, 136, 11100−11106

Table 1. SAXS and TEM Data for (0.40 $PMAA_{62}$ + 0.60 $PMAA_{171}$)-$PBzMA_{312}$, (0.50 $PMAA_{62}$ + 0.50 $PMAA_{171}$)-$PBzMA_{326}$, and $PMAA_{62}$-$PBzMA_{333}$ diblock copolymers synthesized by RAFT Dispersion Polymerization of BzMA at 70°C Using a Binary Mixture of $PMAA_{62}$ and $PMAA_{171}$ macro-CTAs in Ethanol and 20% w/w Solids[a]

				diameter, nm	PDI[c]	membrane thickness, nm	
copolymer composition	copolymer morphology	target DP	actual DP[b]	SAXS	SAXS	TEM[d]	SAXS
(0.4 M_{62} + 0.6 M_{171})-B_{312}	micelles	350	312	62 ± 2.5	0.01	–	–
(0.5 M_{62} + 0.5 M_{171})-B_{326}	vesicles	350	326	199 ± 20	0.05	31 ± 3	29 ± 4
M_{62}-B_{333}	vesicles	350	333	351 ± 60	0.12	~50	38 ± 4

[a]Herein 'M' indicates PMAA, while 'B' denotes PBzMA. [b]Mean DPs for the core-forming PBzMA (or B block) were determined by ^{1}H NMR spectroscopy; [c]Polydispersities (PDI) were calculated as the square of the standard deviation of the diameter divided by the diameter; [d]ImageJ software was used to estimate membrane thicknesses, with data being averaged over 40 vesicles. The mean membrane thickness of the (0.50 $PMAA_{62}$ + 0.50 $PMAA_{171}$)-$PBzMA_{326}$ vesicles was determined from cryo-TEM images (see Figure S6), while conventional TEM images were used for the $PMAA_{62}$-$PBzMA_{333}$ vesicles.

of amorphous carbon. The grids were then plasma glow-discharged for 35 s in order to create a hydrophilic surface. Ethanolic dispersions (0.20% w/w, 10 μL) were then placed onto a freshly glow-discharged grid for 1 min and then blotted with filter paper to remove excess solution. To stain the deposited particles, a 0.75% w/w aqueous solution of uranyl formate (10 μL) was placed via micropipette on a sample-loaded grid for 20 s and then carefully blotted to remove the excess stain. Each grid was then carefully dried using a vacuum hose.

Gel Permeation Chromatography (GPC). The GPC set-up comprised two 5 μm (30 cm) Mixed C columns and a WellChrom K-2301 refractive index detector operating at 950 ± 30 nm. THF eluent containing 2.0% v/v triethylamine and 0.05% w/v butylhydroxytoluene (BHT) was used at a flow rate of 1.0 mL min^{-1}. A series of ten near-monodisperse linear poly(methyl methacrylate) standards (M_p ranging from 1280 to 330,000 g mol^{-1}) were purchased from Agilent (Church Stretton, U.K.) and employed for calibration using the above refractive index detector. Both PMAA macro-CTAs and PMAA-PBzMA diblocks required exhaustive methylation of the methacrylic acid units using excess trimethylsilyldiazomethane.[32]

Dynamic Light Scattering (DLS). DLS measurements were conducted using a Malvern Instruments Zetasizer Nano-ZS instrument equipped with a 4 mW He-Ne laser operating at 633 nm, an avalanche photodiode detector at a fixed angle of 173°, and an ALV/LSE-5003 multiple τ digital correlator electronics system. Autocorrelation functions were analyzed by the cumulants method to calculate the z-average (hydrodynamic) diameter and polydispersity index (PDI).

Small Angle X-ray Scattering (SAXS). SAXS patterns were recorded at two synchrotron sources (ESRF, station ID02, Grenoble, France and Diamond Light Source, station I22, Didcot, U.K.) using monochromatic X-ray radiation (wavelength λ = 0.0995 and 0.1001 nm, respectively) and 2D CCD detectors (FReLoN Kodak and Pilatus 2M, respectively). The camera length set-ups covered q ranges from 0.01 to 1.9 nm^{-1} and from 0.02 to 1.9 nm^{-1}, respectively, where $q = 4\pi \sin\theta/\lambda$ is the modulus of the scattering vector and θ is half of the scattering angle. A liquid cell comprising two mica windows (each of 25 μm thickness) separated by a polytetrafluoroethylene spacer of 1 mm thickness was used as a sample holder. Scattering data reduced by Nika SAS data reduction macros for Igor Pro (integration, normalization and background subtraction) were further analyzed using Irena SAS macros for Igor Pro.[33] The SAXS measurements were conducted on selected ethanolic PMAA-PBzMA copolymer dispersions diluted from the as-synthesized concentrated dispersions to 1.0% w/w solids (Table 1).

RESULTS AND DISCUSSION

Our synthetic strategy is based on the simultaneous chain extension of two hydrophilic macro-CTAs comprising relatively short and long DPs (e.g., $PMAA_{62}$ and $PMAA_{171}$) with a hydrophobic monomer (i.e., BzMA). The GPC traces shown in Figures S1−S3 confirm that the binary mixture PISA formulation is essentially equivalent to the conventional PISA formulation based on the sole $PMAA_{62}$ macro-CTA. In both cases, well-defined diblock copolymer chains with relatively low M_w/M_n values and high blocking efficiencies are obtained, with minimal GPC evidence for macro-CTA contamination. However, using the binary mixture of the two macro-CTAs understandably produces a slightly higher copolymer polydispersity (e.g., an M_w/M_n of 1.36 in Figure S1). Using such a binary mixture of macro-CTAs, two amphiphilic diblock copolymers are generated *in situ* that stabilize differing particle morphologies:[34] $PMAA_{62}$-$PBzMA_x$ favors vesicular self-assembly, while $PMAA_{171}$-$PBzMA_x$ prefers to form spherical micelles (where x is the target DP of the membrane-forming and core-forming PBzMA block respectively; in these experiments x is such that $180 \leq x \leq 350$). According to the literature on the self-assembly of binary mixtures of block copolymers,[18,21,24] the longer $PMAA_{171}$ block should be preferentially located on the outer membrane surface, while the shorter $PMAA_{62}$ block should be expressed at the inner surface. Unlike post-polymerization processing, PISA formulations involve efficient self-assembly at relatively high copolymer concentration, which is a potentially decisive advantage for industrial scale-up. Binary mixtures of chemically different macro-CTAs have been recently explored for PISA formulations.[35,36] However, as far as we are aware the present work is the first to exploit PISA to target relatively small, low-polydispersity vesicles.

Initially, we synthesized a series of $PMAA_{62}$-$PBzMA_x$ (targeting x = 180−350) vesicles at 20% w/w solids in ethanol. DLS and TEM characterization (see Figure S4 and Table S2) confirmed that these vesicles were invariably relatively large and polydisperse, and hence served as a useful reference point (N.B. the PBzMA T_g is ~55 °C, so these vesicles tend to resist collapse under high vacuum). Conversely, small vesicles tended to have relatively narrow size distributions, since the interfacial area (and hence energy) is strongly size dependent.[17] Thus, reducing the vesicle dimensions should simultaneously lower their polydispersity. This hypothesis was examined using DLS, which reports the z-average diameter and polydispersity, to construct a phase diagram (see Figure 1; target PBzMA DP = 350) using various binary mixtures of $PMAA_{62}$ and $PMAA_{171}$ macro-CTAs for the RAFT dispersion polymerization of BzMA in ethanol. Systematic adjustment of the $PMAA_{62}$ mole fraction resulted in copolymer morphologies ranging from small spherical nanoparticles to large vesicles (see Figure 1). Empirically, a $PMAA_{62}$ mole fraction of around 0.50−0.60 offered optimal morphological control. At lower mole fractions, the influence of the major component (i.e., the longer $PMAA_{171}$ block) leads to the formation of spherical nanoparticles, while at relatively high $PMAA_{62}$ mole fractions only rather large, polydisperse vesicles are produced. Moreover, there is a significant reduction in vesicle polydispersity at intermediate $PMAA_{62}$ mole fractions, as judged

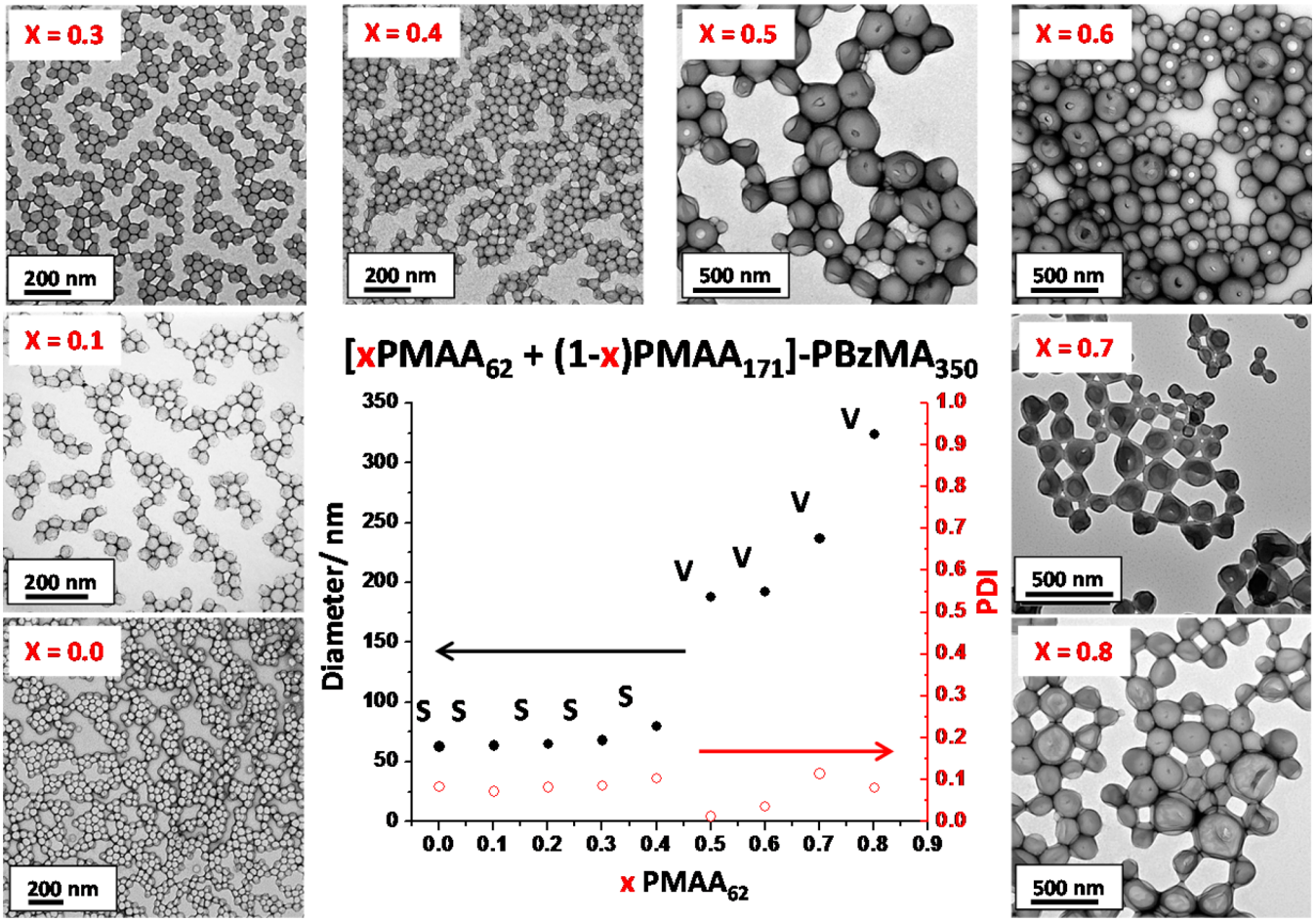

Figure 1. Representative TEM images and corresponding phase diagram determined for $[x\text{PMAA}_{62} + (1 - x)\text{PMAA}_{171}]$-$\text{PBzMA}_{350}$ particles synthesized by RAFT dispersion polymerization of BzMA at 70 °C using a binary mixture of PMAA_{62} and PMAA_{171} macro-CTAs in ethanol at 20% w/w solids. Intensity-average diameters and polydispersities were determined by DLS in ethanol (0.10% w/w solids). **S** indicates spheres and **V** indicates vesicles.

by DLS (see Figure 1). Compared to the reference PMAA_{62}-PBzMA_{350} vesicles (z-average diameter = 405 nm, DLS polydispersity = 0.42), the $(x\text{PMAA}_{62} + (1 - x)\text{PMAA}_{171})$-$\text{PBzMA}_{350}$ vesicles formed at $x = 0.50$ have a significantly lower z-average diameter of 188 nm and a substantially reduced polydispersity of 0.02. These observations are consistent with earlier experimental studies that involved post-polymerization processing of diblock copolymers in dilute aqueous solution,[18] and also with theoretical predictions made by Greenall et al. for the self-assembly of binary mixtures of sphere-forming diblock copolymers with vesicle-forming diblock copolymers.[24] SAXS was utilized to gain further physical insight regarding the morphological transition for the $[x\text{PMAA}_{62} + (1 - x)\text{PMAA}_{171}]$-$\text{PBzMA}_{350}$ formulation on moving from $x = 0.40$ to 0.50. It was found that either a vesicle model or a spherical micelle model (see Supporting Information for descriptions of these two models) produced reasonably good fits to the appropriate SAXS patterns over five orders of magnitude of X-ray scattering intensity (Figure 2). A scattering pattern obtained for the (0.4 PMAA_{62} + 0.6 PMAA_{171})-PBzMA_{312} formulation, with the intensity curve tending toward a zero gradient for $q < 0.1$ nm^{-1}, corresponds to a spherical micelle morphology (see SAXS data in Figure 2a). In contrast, scattering patterns displaying a continuous increase in intensity at $q < 0.1$ nm^{-1} are observed for copolymer dispersions containing a relatively high proportion of the short PMAA_{62} block (see SAXS data in Figures 2b,c). Both these curves can be satisfactorily fitted using the vesicle model. Thus, SAXS data recorded for the ethanolic copolymer dispersions are consistent with TEM studies of the dried copolymer nanoparticles (Figure 2): a sphere-to-vesicle morphological transition occurs between the (0.40 PMAA_{62} + 0.60 PMAA_{171})-PBzMA_{312} and (0.50 PMAA_{62} + 0.50 PMAA_{171})-PBzMA_{326} binary mixture formulations (Figure 1). For the spherical micelle model, it is assumed that the corona is formed by a mixture of uniformly distributed PMAA_{62} and PMAA_{171} blocks, thus an average radius of gyration was used for the model fitting (Table S4). According to Eisenberg and co-workers,[18,19] for vesicles formed by a binary mixture of diblock copolymers comprising essentially the same mean DP for the membrane-forming block, the shorter stabilizer block should be preferentially expressed at the inner leaflet and the longer stabilizer block should be located mainly at the outer leaflet. Such segregation enables the differing packing parameters for the two copolymer chains to be accommodated within the same nano-object. Accordingly, a reasonable approximation that accounts for this localized copolymer segregation is included in the vesicle model used to analyze the SAXS data. Thus two different radii of gyration for the PMAA_{62} and PMAA_{171} blocks ($R_{g\ in}$ and $R_{g\ out}$, respectively, see Supporting Information) were used in the model. An averaged distribution of these blocks across the

dx.doi.org/10.1021/ja505406s | J. Am. Chem. Soc. 2014, 136, 11100−11106

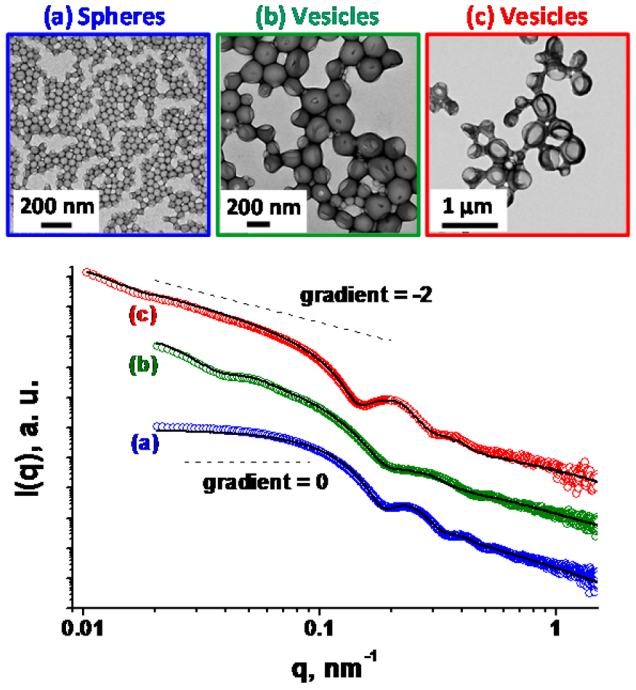

Figure 2. (Upper) Representative TEM images for (a) (0.4 $PMAA_{62}$ + 0.6 $PMAA_{171}$)-$PBzMA_{312}$, (b) (0.5 $PMAA_{62}$ + 0.5 $PMAA_{171}$)-$PBzMA_{326}$, and (c) $PMAA_{62}$-$PBzMA_{333}$ dried copolymer dispersions. (Lower) SAXS patterns obtained for 1.0% w/w copolymer dispersions of: (a) (0.4 $PMAA_{62}$ + 0.6 $PMAA_{171}$)-$PBzMA_{312}$ (blue circles); (b) (0.5 $PMAA_{62}$ + 0.5 $PMAA_{171}$)-$PBzMA_{326}$ (green circles); (c) $PMAA_{62}$-$PBzMA_{333}$ (red circles) in ethanol. Solid lines show fits to the data using a spherical micelle model (a) and a vesicle model (b and c).

membrane was also considered, but the former approach gave a slightly better fit (see SAXS data in Figure 2b and Table S4). The SAXS pattern obtained for the high-polydispersity $PMAA_{62}$-$PBzMA_{333}$ vesicles was fitted using a simplified model such that $R_{g\ in} = R_{g\ out}$ (see SAXS data in Figure 2c and Table S4). SAXS analysis indicates that the average radius of gyration of the PMAA stabilizer blocks is reduced from 3.9 nm for the spherical micelles to 2.9 nm for the polydisperse vesicles formed by the $PMAA_{62}$-$PBzMA_{333}$ alone (Table S4). This is physically reasonable, since the coronal layer of the polydisperse vesicles solely comprises $PMAA_{62}$ chains, whereas the spherical micelles prepared using the binary mixture of macro-CTAs necessarily contains a significant proportion of the longer $PMAA_{171}$ corona-forming block.

In principle, the R_g of the PMAA stabilizer block can be calculated. For example, given that the projected contour length of a single repeat unit in the PMAA block is 0.255 nm (two carbon bonds in an all-trans conformation), the total contour length of the $PMAA_{62}$ block, L = 62 × 0.255 nm =15.83 nm. Assuming a Kuhn length of 1.53 nm [the literature value for poly(methyl methacrylate)[37]] results in an estimated R_g of $(15.83 \times 1.53/6)^{0.5}$, or 2.01 nm. Similarly, the estimated R_g for the $PMAA_{171}$ block is 3.34 nm. However, the R_g values obtained from the SAXS data fits are slightly higher than those calculated. This is reasonable, because the latter values indicate the unperturbed dimensions of the PMAA chains, whereas the experimental data were acquired under better-than-theta solvent (i.e., good solvent) conditions. However, a second possible explanation for the difference between the calculated and fitted R_g value is the uncertainty in the SAXS analysis. A positive correlation between R_g and the volume fraction of ethanol within the membrane (x_{sol}) was observed during such data fitting. Thus reduction of x_{sol} in the model should result in a concomitant reduction in the R_g value.

Close inspection of the SAXS patterns reveals further structural information. Compared to the $PMAA_{62}$-$PBzMA_{333}$ vesicles, the (0.5 $PMAA_{62}$ + 0.5 $PMAA_{171}$)-$PBzMA_{326}$ binary mixture composition exhibits pronounced oscillations in the low q region, which is associated with the overall particle size (compare $q \sim 0.02$ nm^{-1} in Figure 2c, SAXS with $q \sim 0.05$ nm^{-1} in Figure 2b, SAXS). This observation is consistent with DLS data obtained for the same two copolymer dispersions, which indicates that the (0.5 $PMAA_{62}$ + 0.5 $PMAA_{171}$)-$PBzMA_{326}$ binary mixture composition forms vesicles with a significantly lower polydispersity. The particle diameters [calculated for the spherical micelles using $D_s = 2(R_s + 2\bar{R}_g)$ and for the vesicles using $D_v = 2(R_{mc} + 1/2T_{mc} + 2R_{g\ out})$, see Table S4 for definitions of these parameters] and the vesicle membrane thicknesses correlate reasonably well with the TEM data (see Table 1) and also the DLS results. According to the limited data set shown in Table 1 (see entries 2 and 3), SAXS analyses also suggest that an increase in the relative proportion of $PMAA_{62}$ in the binary mixture formulation results in a simultaneous increase in both the overall vesicle diameter and the vesicle membrane thickness. In particular, SAXS confirms that using an optimized binary mixture of $PMAA_{62}$ and $PMAA_{171}$ macro-CTAs enables a remarkable reduction in size and polydispersity to be achieved for PMAA-PBzMA block copolymer vesicles. Since this PISA synthesis is conducted at relatively high solids, it represents the first truly scalable route to provide low-polydispersity vesicles.

In order to support the above experimental studies, we also performed numerical calculations using self-consistent mean-field theory (SCMFT).[37] Over the last two decades SCMFT has become a powerful technique for studying inhomogeneous polymeric systems at equilibrium.[37−39] In particular, it enables thermodynamically preferred self-assembled structures and their associated physical properties to be predicted.[37,38] The central parameter in SCMFT is the mean-field free energy F. In the present study, F incorporates the mixing entropy, the Flory−Huggins mixing enthalpy, the local mean-field interactions (accounting for gradients) and a compressibility constraint.[20] After minimizing this free energy using a self-consistent iterative protocol that does not require information about the equilibrium morphologies, various thermodynamic properties of the resulting equilibrium system can be calculated. In order to perform numerical SCMFT calculations, the block copolymer was subjected to coarse-grain modeling. The three monomeric repeat units are shown in Figure S5, along with other pertinent details. This choice implies that each lattice unit corresponds to approximately 0.5 nm. The interaction energies between the four components were parametrized using χ-parameters in a Flory−Huggins type formalism. These χ-parameters were determined by COSMO-SAC, a thermodynamic model based on quantum mechanical data.[40] The resulting χ-parameters calculated for the RAFT polymerization temperature of 70 °C are listed in Table S5. As expected, the interactions between the benzene group and all other components are rather repulsive. For various conditions, the SCMFT grand potential was computed for differing lattice geometries (flat, cylindrical, or spherical). Suitable conditions were identified for the formation of thermodynamically stable block copolymer vesicles, as observed experimentally. In terms of equilibrium structures, it was verified via SCMFT that $PMAA_{171}$-$PBzMA_{350}$ forms spherical micelles in ethanol at 70 °C, while $PMAA_{62}$-$PBzMA_{350}$ forms vesicles under the same conditions.

dx.doi.org/10.1021/ja505406s | J. Am. Chem. Soc. 2014, 136, 11100−11106

For the computed equilibrium conditions, we calculated and analyzed the volume fraction profiles $\varphi(r)$, with examples being presented in Figure 3 (r is the distance from the center of a vesicle, in lattice units). The results are plotted for the density profiles of all components for the vesicle-forming $PMAA_{62}$-$PBzMA_{350}$ diblock copolymer at a copolymer concentration of 20 vol % (which is close to 20% w/w) in Figure 3a and also for the binary mixture formulation comprising 10 vol % $PMAA_{62}$-$PBzMA_{350}$ and 10 vol % $PMAA_{171}$-$PBzMA_{350}$ in Figure 3b. In both cases a vesicle bilayer is formed, and the profiles in Figure 3a are in agreement with the cartoon structure shown in Scheme 1a. In the case of the binary mixture formulation, the distribution of $PMAA_{62}$ chains between the inner and outer leaflets becomes more asymmetric; the $PMAA_{62}$ blocks tend to become segregated within the vesicle lumen (Figure 3b), as suggested by SAXS model fitting (Figure 2b, SAXS). The differing packing parameters for the $PMAA_{62}$- and $PMAA_{171}$-stabilized diblock copolymers are the driving force that dictates the preferred bilayer curvature.[41,42]

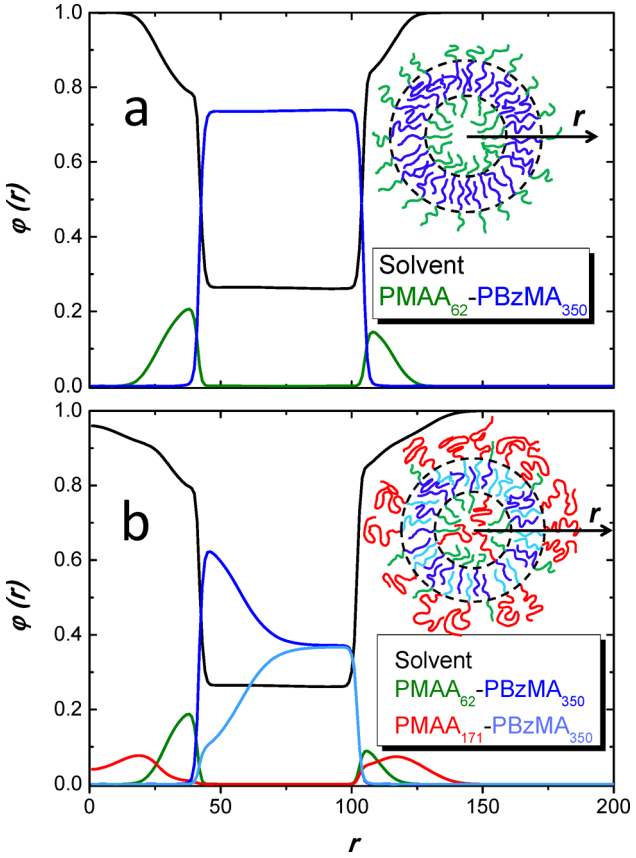

Figure 3. Radial density profiles of volume fraction $\varphi(r)$ vs r (where r is the distance from the center of a vesicle in lattice units, where one lattice unit ≈ 0.5 nm) obtained from SCMFT calculations performed for PMAA-PBzMA diblock copolymer chains in ethanol: (a) vesicles formed by self-assembly of $PMAA_{62}$-$PBzMA_{350}$; (b) vesicles formed by self-assembly of a binary mixture of $PMAA_{62}$-$PBzMA_{350}$ (vesicle-forming) and $PMAA_{171}$-$PBzMA_{350}$ (sphere-forming) diblock copolymers.

Furthermore, the thickness of the external vesicle corona becomes much thicker for the binary mixture formulation, because it is the relatively long $PMAA_{171}$ block that is expressed at the outer vesicle surface and hence mainly protrudes into the bulk solution. Although the binary mixture formulation for low-polydispersity vesicles has a thicker hydrophilic shell, the hydrophobic region layer is slightly thinner (by just a few nm). This is corroborated by the TEM and SAXS data summarized in Table 1, although this effect is somewhat larger for the experimental system. It is noteworthy that SCMFT indicates a similar mean thickness (~ 60 lattice units × 0.5 nm per lattice unit = ~ 30 nm) for the membrane of the low-polydispersity vesicles, see Figure 3b. These theoretical calculations also suggest that the longer $PMAA_{171}$ chains adopt a relatively extended conformation from both the inner and outer membrane surfaces. This is understandable, because if they remained close to the interface, this would increase the local osmotic pressure. On the other hand, both $PMAA_{171}$ and $PMAA_{62}$ are covalently linked to the hydrophobic vesicle membrane. Thus the concentration of both stabilizer blocks should be relatively high at (or near) the membrane surface. In this case the aggregation number for the low-polydispersity vesicles formed using the binary mixture formulation should be lower than that for the high-polydispersity $PMAA_{62}$-$PBzMA_{350}$ reference vesicles. This should result in both a reduction in mean vesicle diameter and also thinning of the vesicle membrane, which is actually observed by TEM and SAXS (see Table 1).

The SCMFT calculations suggest that the solvophobic block is partially plasticized by ethanol (φ ~ 0.3, Figure 3). Indeed, this theoretical prediction is supported by the SAXS analysis, which indicates that the ethanol volume fraction (x_{sol}) is about 0.5 for both the vesicle membranes and the spherical micelle cores (see Table S4).

Low-polydispersity vesicles have also been obtained using several other binary mixtures of macro-CTAs (see Figures S3–S8), thus proving the general applicability of our binary mixture PISA approach. For example, representative TEM images, DLS data and the corresponding phase diagrams are shown in Tables S6–S8 and Figures S7–S12 for binary mixtures of $PMAA_{44}$ + $PMAA_{102}$ and $PMAA_{62}$ + $PMAA_{102}$ macro-CTAs. Close inspection of the DLS polydispersities for various binary mixtures of PMAA macro-CTAs (see Tables S6–S8) indicates an important trend: larger differences between the mean DPs of the macro-CTAs require a higher proportion of the shorter macro-CTA to achieve the minimum vesicle polydispersity. Low-polydispersity vesicles have also been obtained when using chemically dissimilar stabilizer blocks, such as a relatively long PMAA macro-CTA and a relatively short PHPMA macro-CTA (data not shown). In this case, enthalpic incompatibility between the two dissimilar stabilizer blocks is expected to drive even stronger localized segregation across the vesicle membrane. Finally, DLS studies of vesicle dispersions (stored at 20% w/w solids in ethanol prior to dilution) confirm that their particle size and polydispersity remains essentially unchanged after storage at 20 °C for 15 months (e.g., original vesicle diameter = 168 nm, PDI = 0.039; aged vesicle diameter = 164 nm, PDI = 0.024). This indicates that these small low-polydispersity vesicles have excellent long-term colloidal stability.[43]

CONCLUSIONS

In summary, using a binary mixture of a relatively long sphere-forming macro-CTA and a relatively short vesicle-forming macro-CTA enables the convenient synthesis of PMAA-PBzMA diblock copolymer vesicles with relatively narrow size distributions at high solids via polymerization-induced self-assembly using RAFT polymerization. Both SAXS studies and SCMFT calculations indicate that this is achieved by segregation of the PMAA stabilizer blocks, with the longer chains being

expressed at the outer leaflet and the shorter chains being preferentially located at the inner leaflet. This leads to relatively small vesicles comprising a thick outer corona and a thin inner corona, with a significant degree of solvent plasticization of the membrane-forming chains. Moreover, such copolymer segregation leads to a somewhat thinner vesicle membrane compared to that found for the relatively polydisperse vesicles obtained when using the shorter PMAA block as the sole stabilizer. This facile self-assembly strategy is amenable to industrial scale-up and is expected to be of rather general utility.

■ ASSOCIATED CONTENT

Supporting Information

Synthetic details for the PMAA-based macro-CTAs used in this study, GPC curves for macro-CTAs and diblock copolymers, detailed spherical micelles and vesicle SAXS models, six further diblock copolymer phase diagrams based on DLS data with corresponding TEM images. This material is available free of charge via the Internet at http://pubs.acs.org.

■ AUTHOR INFORMATION

Corresponding Authors

s.p.armes@sheffield.ac.uk
O.Mykhaylyk@sheffield.ac.uk

Notes

The authors declare no competing financial interest.

■ ACKNOWLEDGMENTS

We are grateful to Diamond Light Source for providing synchrotron beam-time and thank the personnel of I22 for their assistance. We also acknowledge ESRF for their beam-time allocation and wish to thank the personnel of ID02 station for their help with SAXS experiments described herein. We thank DSM Advanced Surfaces (Geleen, The Netherlands) for postdoctoral support of C.G. and M.S., EPSRC for a Platform grant to support O.O.M. (EP/J007846/1), and the ERC for an Advanced Investigator grant for SPA (PISA 320372). The three reviewers of this manuscript are also thanked for their constructive criticisms.

■ REFERENCES

(1) Zhang, L.; Eisenberg, A. *Science* **1995**, *268*, 1728.
(2) Zhang, L.; Eisenberg, A. *J. Am. Chem. Soc.* **1996**, *118*, 3168.
(3) Brinkhuis, R. P.; Rutjes, F. P.; van Hest, J. C. *Polym. Chem.* **2011**, *2*, 1449.
(4) Brannan, A. K.; Bates, F. S. *Macromolecules* **2004**, *37*, 8816.
(5) Discher, D. E.; Ortiz, V.; Srinivas, G.; Klein, M. L.; Kim, Y.; Christian, D.; Cai, S.; Photos, P.; Ahmed, F. *Prog. Polym. Sci.* **2007**, *32*, 838.
(6) Choe, U.-J.; Sun, V.; Tan, J.-K.; Kamei, D. In *Peptide-Based Materials*; Deming, T., Ed.; Springer: Berlin, Heidelberg, 2012; Vol. *310*, p 117.
(7) Le Meins, J.-F.; Sandre, O.; Lecommandoux, S. *Eur. Phys. J. E* **2011**, *34*, 1.
(8) Bangham, A.; Horne, R. *J. Mol. Biol.* **1964**, *8*, 660.
(9) Discher, B. M.; Won, Y.-Y.; Ege, D. S.; Lee, J. C.; Bates, F. S.; Discher, D. E.; Hammer, D. A. *Science* **1999**, *284*, 1143.
(10) Hayward, R. C.; Pochan, D. J. *Macromolecules* **2010**, *43*, 3577.
(11) Chen, L.; Shen, H.; Eisenberg, A. *J. Phys. Chem. B* **1999**, *103*, 9488.
(12) Pereira-Lachataignerais, J.; Pons, R.; Panizza, P.; Courbin, L.; Rouch, J.; López, O. *Chem. Phys. Lipids* **2006**, *140*, 88.
(13) Rank, A.; Hauschild, S.; Förster, S.; Schubert, R. *Langmuir* **2009**, *25*, 1337.
(14) Brandl, M.; Bachmann, D.; Drechsler, M.; Bauer, K. *Drug Dev. Ind. Pharm.* **1990**, *16*, 2167.
(15) Howse, J. R.; Jones, R. A.; Battaglia, G.; Ducker, R. E.; Leggett, G. J.; Ryan, A. J. *Nat. Mater.* **2009**, *8*, 507.
(16) Hauschild, S.; Lipprandt, U.; Rumplecker, A.; Borchert, U.; Rank, A.; Schubert, R.; Förster, S. *Small* **2005**, *1*, 1177.
(17) Mai, Y.; Eisenberg, A. *Chem. Soc. Rev.* **2012**, *41*, 5969.
(18) Terreau, O.; Luo, L.; Eisenberg, A. *Langmuir* **2003**, *19*, 5601.
(19) Luo, L.; Eisenberg, A. *J. Am. Chem. Soc.* **2001**, *123*, 1012.
(20) Li, F.; Marcelis, A. T. M.; Sudholter, E. J. R.; Cohen Stuart, M. A.; Leermakers, F. A. M. *Soft Matter* **2009**, *5*, 4173.
(21) Li, F.; Prevost, S.; Schweins, R.; Marcelis, A. T. M.; Leermakers, F. A. M.; Cohen Stuart, M. A.; Sudholter, E. J. R. *Soft Matter* **2009**, *5*, 4169.
(22) Schuetz, P.; Greenall, M. J.; Bent, J.; Furzeland, S.; Atkins, D.; Butler, M. F.; McLeish, T. C. B.; Buzza, D. M. A. *Soft Matter* **2011**, *7*, 749.
(23) Greenall, M. J.; Schuetz, P.; Furzeland, S.; Atkins, D.; Buzza, D. M. A.; Butler, M. F.; McLeish, T. C. B. *Macromolecules* **2011**, *44*, 5510.
(24) Greenall, M. J.; Gompper, G. *Macromolecules* **2011**, *45*, 525.
(25) Greenall, M. J.; Marques, C. M. *Phys. Rev. Lett.* **2013**, *110*, 088301.
(26) Jain, S.; Bates, F. S. *Macromolecules* **2004**, *37*, 1511.
(27) Stoenescu, R.; Meier, W. *Chem. Commun.* **2002**, 3016.
(28) Charleux, B.; Delaittre, G.; Rieger, J.; D'Agosto, F. *Macromolecules* **2012**, *45*, 6753.
(29) Blanazs, A.; Verber, R.; Mykhaylyk, O. O.; Ryan, A. J.; Heath, J. Z.; Douglas, C. W. I.; Armes, S. P. *J. Am. Chem. Soc.* **2012**, *134*, 9741.
(30) Semsarilar, M.; Jones, E. R.; Blanazs, A.; Armes, S. P. *Adv. Mater.* **2012**, *24*, 3378.
(31) Sun, J.-T.; Hong, C.-Y.; Pan, C.-Y. *Polym. Chem.* **2013**, *4*, 873.
(32) Graham, S.; Cormack, P. A.; Sherrington, D. C. *Macromolecules* **2005**, *38*, 86.
(33) Ilavsky, J.; Jemian, P. R. *J. Appl. Crystallogr.* **2009**, *42*, 347.
(34) Israelachvili, J. N.; Mitchell, D. J.; Ninham, B. W. *J. Chem. Soc., Faraday Trans. 2* **1976**, *72*, 1525.
(35) Semsarilar, M.; Ladmiral, V.; Blanazs, A.; Armes, S. P. *Langmuir* **2012**, *28*, 914.
(36) Semsarilar, M.; Ladmiral, V.; Blanazs, A.; Armes, S. *Langmuir* **2013**, *29*, 7416.
(37) Fetters, L. J.; Lohsey, D. J.; Colby, R. H. In *Physical Properties of Polymers Handbook*, 2nd ed.; Mark, J. E., Ed.; Springer: New York, 2007; p 447.
(38) Fleer, G. J.; Cohen Stuart, M. A.; Scheutjens, J. M. H. M.; Cosgrove, B.; Vincent, B. *Polymers at interfaces*; Springer: New York, 1993.
(39) Fredrickson, G. H.; Ganesan, V.; Drolet, F. *Macromolecules* **2002**, *35*, 16.
(40) Claessens, M.; Van Oort, B.; Leermakers, F. A. M.; Hoekstra, F.; Cohen Stuart, M. A. *Biophys. J.* **2004**, *87*, 3882.
(41) Mullins, E.; Oldland, R.; Liu, Y.; Wang, S.; Sandler, S. I.; Chen, C.-C.; Zwolak, M.; Seavey, K. C. *Ind. Eng. Chem. Res.* **2006**, *45*, 4389.
(42) Lin, C.-M.; Li, C.-S.; Sheng, Y.-J.; Wu, D. T.; Tsao, H.-K. *Langmuir* **2012**, *28*, 689.
(43) Leermakers, F. A. M.; Eriksson, J. C.; Lyklema, J. *Association colloids and their equilibrium modelling, Fundamentals in Colloid and Interface Science*; Elsevier: Amsterdam, 2005; Vol. *5*.